

Recently, many deep learning (DL)-based image resolution enhancement methods have been developed and have shown a notable performance. However, due to the lack of an appropriate training dataset and a necessity of high computing power, a successful application to skeletal image enhancement has not been reported. To overcome a difficulty of obtaining a training dataset, the topology optimization (TO)-based resolution enhancement method (J. J. Kim et al., 2018) can be utilized to generate high-resolution (HR) skeletal images. Note that topology optimization has successfully determined the optimal bone spatial distribution in the proximal femur, but this method consumes extreme computing cost.

This paper proposes a novel framework which incorporates topology optimization and deep learning to enhance a large-size low-resolution (LR) skeletal image. First of all, topology optimization generates 2D synthetic femur images of a $50\mu\text{m}$ resolution under a different total bone mass and loading conditions. These HR images were then downscaled into the corresponding LR image of a $500\mu\text{m}$ resolution. Then, the structural behavior of the LR images was obtained by conducting the finite element (FE) analysis. A pair of the LR- and HR-images and the structural behavior map were divided into small images patches to construct the training dataset for a neural network. Residual network (ResNet) (C. Dong et al., 2014) was used in this study. The reconstructed HR images were then seamlessly quilted into a full proximal femur image. They were evaluated at three different regions of interest (ROIs) in terms of apparent stiffness to assess the performance of each network used in this study.

2. PROPOSED IMAGE RESOLUTION ENHANCEMENT FRAMEWORK

The proposed method consists of the following three steps. First, the LR full proximal femur image is divided into a set of small image patches. Then, the image patches are reconstructed through the trained deep neural network. Finally, the reconstructed HR image patches are seamlessly connected to a HR full proximal femur image (Fig 1). The details are explained in the following sections.

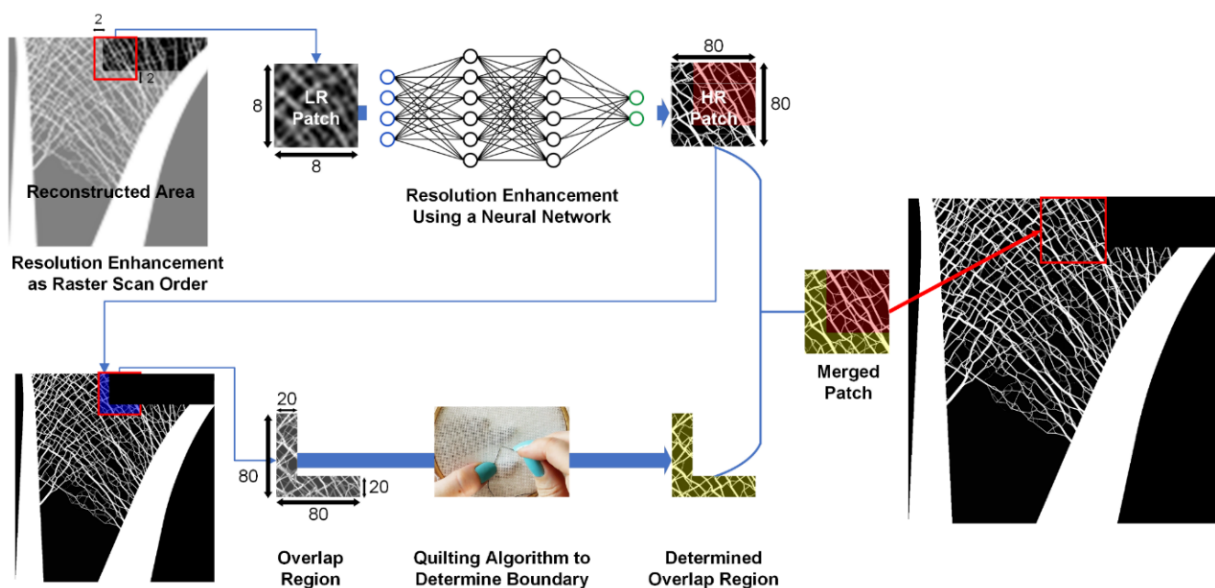


Fig 1. Overall flow of the proposed framework

2.1 Training data generation

Topology optimization was conducted to generate eleven 2D synthetic femur images (1883×2080 with 50μm resolution) as the reference HR femur image. Each femur image was generated under a different total bone mass constraint and loading set. The HR femur images were downscaled 10 times to obtain the LR femur images of a 500μm resolution. Then, the FEA was conducted to obtain the displacement field of the LR images. Note that the image patches were extracted to have an overlapped region among the patches. A total of 547,456 image pairs from 7 femur images were used as the training and validation set, and 312,832 image pairs from the remaining 4 femur images were used as the test set.

2.2 Neural network training

ResNet with MAE (L1) and MSE (L2) losses was trained using the constructed dataset. Each loss function can be expressed, as follows:

$$L_{MAE} = \frac{1}{N^2} \sum_{x=1}^N \sum_{y=1}^N |I_{x,y}^{HR} - G_{\theta_G}(I^{LR})_{x,y}|^2 \quad (1)$$

$$L_{MSE} = \frac{1}{N^2} \sum_{x=1}^N \sum_{y=1}^N (I_{x,y}^{HR} - G_{\theta_G}(I^{LR})_{x,y})^2 \quad (2)$$

where I^{HR} and I^{LR} denote the bone mass distribution of the HR and LR image patches, respectively; G_{θ_G} is the generator network parametrized by θ_G , and N is the side length of the HR image patches in pixels.

2.3 Quilting algorithm of the reconstructed HR image patches

The minimum error path in the overlapped region was determined by Dijkstra's algorithm (Dijkstra, 1959). The determined minimum error path was utilized as a new boundary of mating patches to generate the filling masks between the adjacent two patches.

3.RESULT

Figure 3 shows that the reconstructed femur image has similar trabecular architecture compared with the reference image. All characteristic trabecular patterns were observed in the three ROIs: femoral head, femoral neck, and intertrochanteric region. ResNet with a L2 loss showed a better structural similarity although there exist blurry parts, whereas ResNet with a L1 loss showed a clearer image with more trabecular disconnections.

The apparent stiffness of the reconstructed images is listed in Table 1. ResNet with a L2 loss showed a better apparent stiffness accuracy. Note that all apparent stiffnesses

were underestimated due to the trabecular disconnection. Although a trabecular disconnection remains inside the patch, the proposed quilting algorithm makes the structural discontinuity between the patches minimized (Fig. 3).

The entire reconstruction process consumes only 0.15 hours in total. Note that the neural network training process takes 15.2 hours and 14.8 hours for the ResNet with L1 and L2 losses, respectively. All computation was performed on the PC (Ryzen 5800X, 64GB RAM and GTX1080ti).

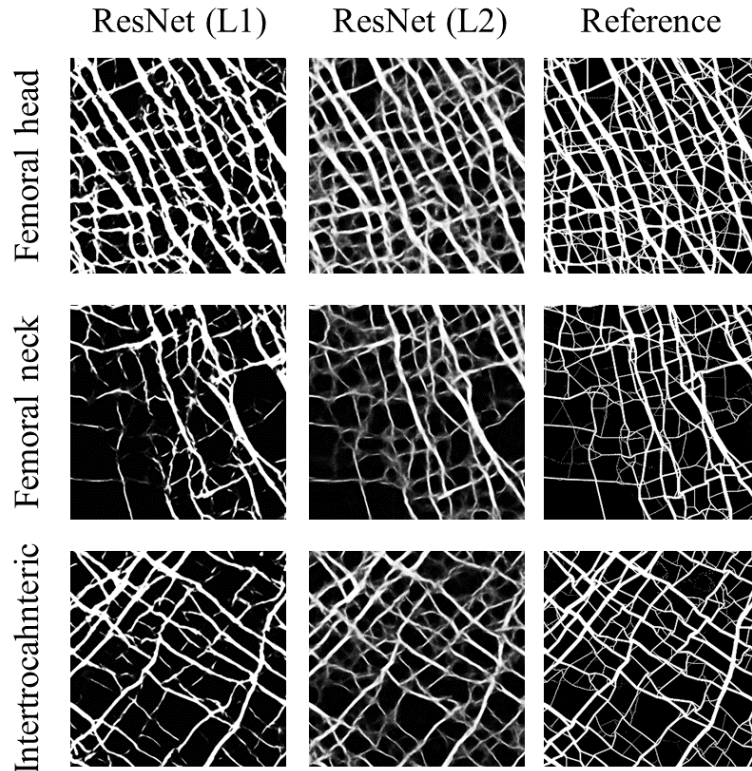


Fig 2. Reconstructed trabecular structure for the ROIs

Table 1. Average errors of apparent stiffness for the ROIs

Region of interest	Stiffness	Apparent stiffness error [%]	
		ResNet (L1 loss)	ResNet (L2 loss)
Femoral head	E_x	83.84	55.35
	E_y	72.88	42.92
	E_{xy}	81.13	30.73
Femoral neck	E_x	98.67	69.13
	E_y	91.17	57.13
	E_{xy}	95.66	55.41
Intertrochanteric region	E_x	92.38	36.88
	E_y	96.99	49.22
	E_{xy}	97.79	44.15

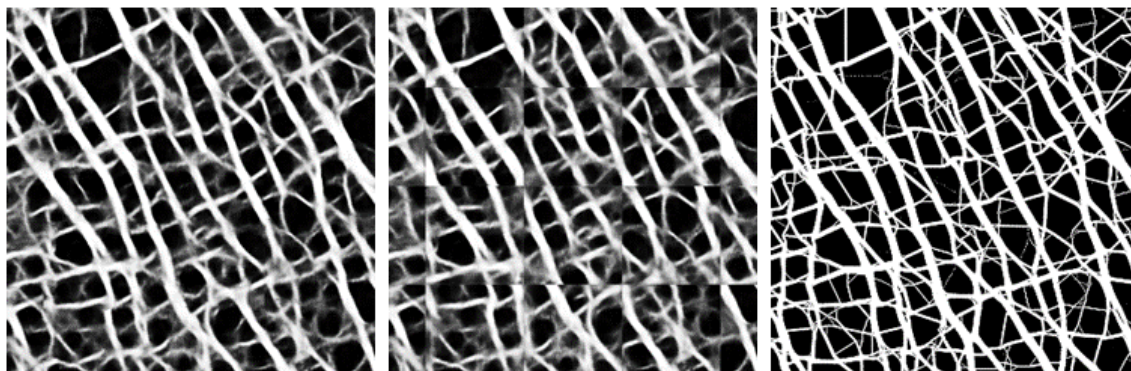


Fig 3. Comparison of reconstructed trabecular structures by the proposed method (left), the proposed method without quilting (middle), and the reference (right)

4.CONCLUSIONS

This study proposed a novel framework for image solution enhancement through the patchwise reconstruction and quilting. Using 860,288 image patches generated by topology optimization, the deep neural network was successfully trained to reconstruct a full proximal femur image of 1883×2080. Once the deep neural network for the patchwise reconstruction is trained, the proposed framework allows for bone microstructure reconstruction within a shorter timeframe and thus contributes to developing a reliable tool for bone health assessment.

AKNOWLEDGEMENT

This work was supported by the National Research Foundation of Korea (NRF) grant funded by the Korea Government (MSIT) (2021R1A2C2009860).

REFERENCES

- Ammann, P., & Rizzoli, R. (2003). Bone strength and its determinants. *Osteoporosis International*, 14(S3), 13–18. <https://doi.org/10.1007/s00198-002-1345-4>
- Dijkstra, E. W. (1959). A note on two problems in connexion with graphs. *Numerische Mathematik*, 1(1), 269–271. <https://doi.org/10.1007/BF01386390>
- Dong, C., Loy, C. C., He, K., & Tang, X. (2014). Image Super-Resolution Using Deep Convolutional Networks. <http://arxiv.org/abs/1501.00092>
- Goldstein, S. A., Goulet, R., & McCubbrey, D. (1993). Measurement and significance of three-dimensional architecture to the mechanical integrity of trabecular bone. *Calcified Tissue International*, 53(1 Supplement), S127–S133. <https://doi.org/10.1007/BF01673421>
- Kim, J. J., Nam, J., & Jang, I. G. (2018). Computational study of estimating 3D trabecular bone microstructure for the volume of interest from CT scan data. *International Journal for Numerical Methods in Biomedical Engineering*, November, 1–13. <https://doi.org/10.1002/cnm.2950>